Wood's anomalies for arrays of dielectric scatterers

A. Maurel Institut Langevin CNRS ESPCI ParisTech, 1 rue Jussieu 75005 Paris France
agnes.maurel@espci.fr

S. Félix LAUM CNRS Université du Maine, avenue Olivier Messiaen 72085 Le Mans France

J.-F. Mercier Poems CNRS ENSTA ParisTech INRIA, 828 boulevard des Maréchaux 91762 Palaiseau France

A. Ourir Institut Langevin CNRS ESPCI ParisTech, 1 rue Jussieu 75005 Paris France

Z. E. Djeffal Institut Langevin CNRS ESPCI ParisTech, 1 rue Jussieu 75005 Paris France

The Rayleigh Wood anomalies refer to an unexpected repartition of the electromagnetic energy between the several interference orders of the light emerging from a grating. Since Hessel and Oliner (Appl. Opt. **4**, 1275-1297 (1965)), several studies have been dedicated to this problem, focusing mainly on the case of metallic gratings. In this paper, we derive explicit expressions of the reflection coefficients in the case of dielectric gratings using a perturbative approach. This is done in a multimodal description of the field combined with the use of the admittance matrix, analog to the so-called electromagnetic impedance. Comparisons with direct numerical calculations show a good agreement with our analytical prediction.
[DOI: http://dx.doi.org/10.2971/jeos.2014.14001]

Keywords: Wood anomalies, admittance matrix, coupled wave analysis

1 INTRODUCTION

Wood's anomalies are concerned with the reflection spectrum of a light source on a periodic metallic grating. Wood noticed that around certain frequencies, the reflectance experienced sudden and intense variations even for small grating grooves. These sudden variations are unexpected if one refers to the reflectance of the flat metallic surface, for which the grooves can be considered as small perturbations. If the main features of the two anomalies have been captured in the paper of Hessel and Oliner [1] (see also [2]–[4]), quantitative predictions of the reflection spectrum, even approximate, are still lacking. As pointed out in a review by Maystre [5], this is because one needs the electromagnetic impedance Y on a straight line located above the grating grooves to be determined. In fact, it is possible in general to calculate Y by solving the associated Riccati equation [6, 7]. Alternatively, in [8], the problem is solved by determining the complex poles of the scattering matrix. Although accurate, these approaches do not provide simple analytical expressions of the reflection coefficients. This is the aim of the present study to provide such expressions. To do that, we derive the impedance matrix perturbatively with respect to a reference, and close, situation where the anomalies do not occur and where the impedance matrix is known. For simplicity, we consider here the case of a dielectric grating as sketched in Figure 1. The scatterers in the periodic row are assumed weak, so that the reference situation is the free space (zero reflection), and the reference impedance is known. Then, the impedance of the grating is determined by solving the linearized version of the Riccati equation and by inverting the system proposed in Hessel and Oliner. Although more involved, the case of a metallic grating can be treated in a similar way: the reference would be the flat interface metal/air, and the perturbation the small grooves.

Our configuration is sketched in Figure 1: a plane wave impinging at normal incidence on an infinite periodic row of scatterers with permittivity $\epsilon > 1$ and permeability $\mu = 1$; the host medium is the free space. The wave equation for transverse electric (TE, or s-polarized light) is

$$\nabla \cdot (\nabla E(\mathbf{r})) + \epsilon(\mathbf{r}) k^2 \, E(\mathbf{r}) = 0, \tag{1}$$

with E the electric field, k^2 the wavenumber in free space, and $\epsilon(\mathbf{r})$ stands for ϵ in the scatterer and for unity in the host medium. This case will be considered in details since it is the polarization for which anomalies are found (contrary to the case of metallic grating). For transverse magnetic waves (TM, or p-polarized), it is

$$\nabla \cdot \left(\frac{1}{\epsilon(\mathbf{r})} \nabla H(\mathbf{r}) \right) + k^2 \, H(\mathbf{r}) = 0, \tag{2}$$

with H the magnetic field, and it is shown in Appendix A that no anomaly occurs, for weak scattering strength.

Received October 18, 2013; resubmitted ms. accepted December 03, 2013; published January 08, 2014 ISSN 1990-2573

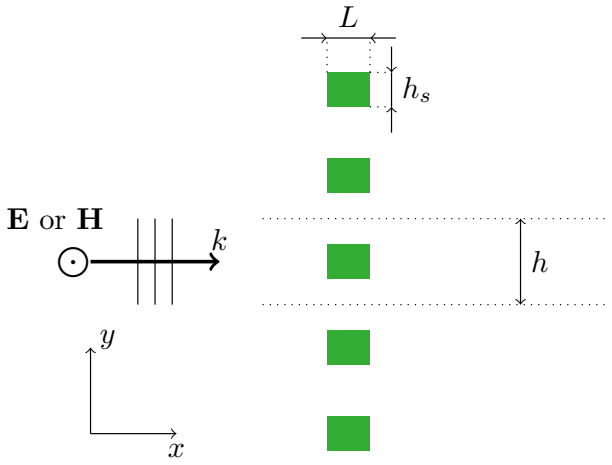

FIG. 1 Geometry and notation of the scattering problem.

2 POSITION OF THE PROBLEM

In this section, the derivation of the coupled mode equations is briefly presented, and the Riccati equation governing the impedance is derived. Then, the system used by Hessel and Oliner [1] to analyze the scattering problem is considered. This system originally uses the electromagnetic impedance Y and it is rewritten here in terms of z, a quantity related to $\mathsf{y} = \mathsf{Y} - \mathsf{Y}^{(0)}$, the deviation in the impedance with respect to the impedance in the absence of scatterers, $\mathsf{Y}^{(0)}$. The system (15) together with the resolution of the Riccati equation (13) is the key point of the presented study.

2.1 The Riccati equation on the impedance matrix for TE waves

Because of the symmetry of our configuration (Figure 1), the problem is equivalent to a single scatterer centered in a waveguide with Neumann boundary conditions on the walls $y = 0, h$. The electric field $E(x,y)$ is expanded as

$$E(x,y) = \sum_{m=0}^{N-1} E_m(x)\varphi_m(y), \tag{3}$$

with $\{\varphi_m\}$ the natural basis of transverse even functions of the Neumann waveguide

$$\varphi_m(y) \equiv \sqrt{\frac{2-\delta_{m0}}{h}} \cos\left(2m\pi\frac{y}{h}\right). \tag{4}$$

We also define

$$k_m^2 \equiv k^2 - \left(\frac{2m\pi}{h}\right)^2. \tag{5}$$

The odd transverse functions are omitted because of the symmetry but, to be consistent with the usual convention, we call mode 0, 2, ... the even modes defined here for $m = 0, 1, \ldots$ Following [9, 10], the wave Eq. (1) is written in a weak formulation

$$\int_\Omega \mathrm{d}\mathbf{r}\left[\nabla E\cdot\nabla\tilde{E} - k^2 E\tilde{E}\right] - k^2(\epsilon-1)\int_{\Omega_0}\mathrm{d}\mathbf{r}\, E\tilde{E} = 0, \tag{6}$$

where $\tilde{E}(\mathbf{r}) = \tilde{E}(x)\varphi_n(y)$ is a test function compactly supported, Ω and Ω_0 denote respectively the whole space of the waveguide and the space occupied by the penetrable scatterers, and it is easy to deduce

$$E_n'' + k_n^2 E_n + k^2(\epsilon-1)\,\mathsf{C}_{nm}E_m = 0, \tag{7}$$

where the Einstein summation convention is used and prime denotes the derivative with respect to x. The matrix C has elements C_{nm}, with

$$\mathsf{C}_{nm}(x) \equiv \int_{(h-h_s)/2}^{(h+h_s)/2} \mathrm{d}y\,\varphi_n(y)\varphi_m(y) \tag{8}$$

for all x where there is a scatterer, and $\mathsf{C}_{nm} = 0$ otherwise.

Defining the quantity $F_n \equiv E_n'$, the above equation can be written as a set of first-order coupled equations governing the modal components $\mathbf{E} \equiv (E_m)$ and $\mathbf{F} \equiv (F_m)$:

$$\begin{pmatrix}\mathbf{E}\\ \mathbf{F}\end{pmatrix}' = \begin{pmatrix}0 & \mathsf{I}\\ \mathsf{K}^2+\mathsf{M} & 0\end{pmatrix}\begin{pmatrix}\mathbf{E}\\ \mathbf{F}\end{pmatrix} \tag{9}$$

where I is the identity matrix, K is a diagonal matrix with $\mathsf{K}_n = ik_n$ and the matrix M is defined by

$$\mathsf{M}(x) \equiv -k^2(\epsilon-1)\,\mathsf{C}(x). \tag{10}$$

Note that the above system can be obtained by projecting directly the wave equation (1) onto the φ_n functions. However, in the case of TM waves (see Appendix A), the weak formulation allows to naturally take into account the exact boundary condition at the scatterer boundaries.

Now, we define the admittance matrix, that links the vector $\mathbf{F}$ to $\mathbf{E}$: $\mathbf{F} = \mathsf{Y}\mathbf{E}$ (it is close to the usual electromagnetic impedance). Using (9), the admittance matrix satisfies a Riccati equation,

$$\mathsf{Y}' = -\mathsf{Y}^2 + \mathsf{K}^2 + \mathsf{M}, \tag{11}$$

that has to be integrated from the output ($x = L$) to the input ($x = 0$) of the region of interest, given an initial condition $\mathsf{Y}(L)$. Since the region $x > L$ is such that only right-going waves can propagate (the medium is uniform and contains no source), $\mathsf{M}(x > L) = 0$ and thus, from Eq. (9), $\mathbf{E}' = \mathbf{F}$ and $\mathbf{F}' = \mathsf{K}^2\mathbf{E}$. It follows that $\mathsf{Y}(L) = \mathsf{K}$. The resolution of Y is a key point of our method, but rather than Y, the problem is written in terms of another (and related) quantity z. We first define the impedance matrix in the absence of grating: here, it is simply $\mathsf{Y}^{(0)} = \mathsf{K}$ for all x-value. Then, the Ricatti equation (11) is rewritten in terms of the quantity z

$$\mathsf{y} \equiv \mathsf{Y} - \mathsf{K}, \quad \text{and} \quad 2\mathsf{z} \equiv \mathsf{K}^{-1}\mathsf{y} \tag{12}$$

where y represents the deviation in the impedance with respect to the empty guide. We get

$$\mathsf{z}' = -2\mathsf{z}\mathsf{K}\mathsf{z} - \mathsf{K}\mathsf{z} - \mathsf{z}\mathsf{K} + \mathsf{K}^{-1}\mathsf{M}/2, \tag{13}$$

and a linearized version of this equation will be used in the following.

2.2 Matrix system on the reflection coefficients

Now, we want to analyze the reflected wave field in the region $x \leq 0$. In this region, the field is written

$E = E^r + E^{inc}$, the sum of the incident and reflected wave, we have $\partial_x E_n = ik_n(E_n^{inc} - E_n^r)$, and by definition $\partial_x E_n = \mathsf{Y}_{nm}E_m$. The system can be written

$$[\mathsf{K}+\mathsf{Y}]\,\mathbf{E}^r = [\mathsf{K}-\mathsf{Y}]\,\mathbf{E}^{inc}, \tag{14}$$

which is equivalent to the one used in [1] for the total field $[\mathsf{K}+\mathsf{Y}]\,\mathbf{E} = 2\mathsf{K}\mathbf{E}^{inc}$. In our case, $E_n^{inc} = \delta_{n0}$ since the incident wave is a plane wave, and the components E_n^r are simply the reflection coefficients, denoted R_n in the following. The system in Eq. (14) can be written as a function of z: $(\mathsf{I}+\mathsf{z})\mathbf{E}^r = -\mathsf{z}\mathbf{E}^{inc}$, explicitly

$$\begin{bmatrix} 1+\mathsf{z}_{00} & \mathsf{z}_{01} & \cdots & \mathsf{z}_{0N} \\ \mathsf{z}_{10} & 1+\mathsf{z}_{11} & & \vdots \\ \vdots & & \ddots & \\ \mathsf{z}_{N0} & \cdots & & 1+\mathsf{z}_{NN} \end{bmatrix} \begin{bmatrix} \mathsf{R}_0 \\ \mathsf{R}_1 \\ \vdots \\ \mathsf{R}_N \end{bmatrix} = \begin{bmatrix} -\mathsf{z}_{00} \\ -\mathsf{z}_{10} \\ \vdots \\ -\mathsf{z}_{N0} \end{bmatrix}, \tag{15}$$

and in the system above, z_{nm} stands for $\mathsf{z}_{nm}(0)$.

At this point, it is clear that the resolution of Eq. (13) and (15) would give the exact solution for the reflected field; it is actually a possible way to derive the reflection matrix in numerical modal methods [10]. Nevertheless, the resolution of the system is not possible analytically in general, and not in our particular case. We present in the following section a way to derive an approximate solution in the weak scattering approximation.

3 APPROXIMATE SOLUTIONS IN THE WEAK SCATTERING APPROXIMATION

We will use mainly two approximations, both being related to the hypothesis of weak scattering. The weak scattering is measured by a small parameter $Z \ll 1$, and Z will be defined later, Eq. (18). Firstly, the Riccati equation (13) is linearized for small $\mathsf{z} = \mathcal{O}(Z)$, which allows to get an approximation of the matrix z, Eqs. (17). When this is done, the reflection coefficients can be obtained by inverting numerically the system (15) truncated at some order N. We refer to these coefficients as the exact solution of the linearized problem, $\mathsf{R}_n^{(2)}$. Alternatively, and to get explicit expressions of R, the system (15) is inverted at dominant order in Z and we use a sort of trick to do that. This gives an estimate of the reflection coefficient, referred as $\mathsf{R}_n^{(1)}$. To anticipate, it will be shown that $\mathsf{R}_n^{(1)} \simeq \mathsf{R}_n^{(2)}$, which means that the main error is due to the linearization of the Riccati equation (13).

3.1 Linearization of the Riccati equation

The linearization of Eq. (13) simply consists in neglecting the non linear term zKz, from which the resulting system is nicely decoupled, and each z_{nm} satisfies (here the Einstein summation convention does not apply)

$$\mathsf{z}'_{nm} = -i(k_n+k_m)\mathsf{z}_{nm} + \frac{\mathsf{M}_{nm}}{2ik_n}. \tag{16}$$

Since $\mathsf{z}_{nm}(L) = 0$, the solution is, at dominant order $\mathsf{z}_{nm}(0) = -\mathsf{M}_{nm}L/(2ik_n)$, and using $\mathsf{C}_{nm} \simeq h_s\varphi_n(h/2)\varphi_m(h/2)$ in Eq. (8), we get at dominant order (for small scatterer size)

$$\mathsf{z}_{nm} \simeq -i\alpha_{nm}\frac{k}{k_n}Z, \tag{17}$$

where we have defined

$$\begin{cases} \alpha_{nm} \equiv \dfrac{(-1)^{(n+m)}}{2}\sqrt{2-\delta_{n0}}\sqrt{2-\delta_{m0}}, \\ Z \equiv (\epsilon-1)kL\dfrac{h_s}{h}, \end{cases} \tag{18}$$

and where the small parameter Z appears to be a balance between weak contrast, low frequency regime and small size scatterer. If the convergence of the series (that is large m and n values) is regarded, a shape factor has to be considered, that results from an exact calculation of C_{nm} and exact integration of the linearized Riccati equation, namely

$$\mathsf{z}_{nm} = -i\alpha_{nm}(k/k_n)Z\mathcal{S}_{nm} \tag{19}$$

with

$$\mathcal{S}_{nm} \equiv \left[\operatorname{sinc}\frac{(n-m)\pi h_s}{h} + \operatorname{sinc}\frac{(n+m)\pi h_s}{h}\right] \times \frac{e^{i(k_n+k_m)L}-1}{2i(k_n+k_m)L}, \tag{20}$$

where we defined $\operatorname{sinc}x \equiv \sin x/x$.

3.2 Approximate inversion of system (15)

As previously said, once z is known, the system (15) can be inverted numerically for any N values. This can be done using Eq. (17) for moderate N-values, typically $k_N L, Nh_s/h \ll 1$ or by explicitly taking into account the shape factors. Alternatively, one can look for an expression for R_n at dominant order in Z. To do that, we use a trick: indeed, because we are looking for sudden variations of R_n, we want to avoid the trivial estimate $\mathsf{R}_n = -\mathsf{z}_{n0}$. Rather, we want to determine under which condition one observes a deviation with respect to this simple behavior. To do that, we first determine the determinant $\Delta \equiv det(\mathsf{I}+\mathsf{z})$ of the matrix to be inverted, at dominant order, linear in Z

$$\Delta = 1 + \sum_j \mathsf{z}_{jj}. \tag{21}$$

The system is then solved by looking for a solution of the form

$$\mathsf{R}_n = \frac{r_n}{\Delta}, \tag{22}$$

and here, we expect $r_n = \mathcal{O}(Z)$. It follows that the system to be solved is

$$r_n + \sum_j \mathsf{z}_{nj}r_j = -(1+\sum_j \mathsf{z}_{jj})\mathsf{z}_{n0}, \tag{23}$$

from which we deduce at dominant order $r_n = -z_{n0}$, and thus,

$$\mathsf{R}_n \simeq -\frac{\mathsf{z}_{n0}}{1+\sum_j \mathsf{z}_{jj}}. \tag{24}$$

Incidentally, note that the convergence of the series $\sum_j \mathsf{z}_{jj}$ can be addressed. We have $\mathsf{z}_{jj} = -i\alpha_{jj}Z(k/k_j)\ \mathcal{S}_{jj}$ and for large j, $\mathcal{S}_{jj} \propto 1/k_j$ from Eq. (20); it follows that $\mathsf{z}_{jj} \propto 1/k_j^2 \sim 1/j^2$, and the series indeed converges.

There are two situations where R_n may deviate from the behavior $\mathcal{O}(Z)$ and these situations correspond to Wood's anomalies. Near $k_m = 0$, both z_{m0} and z_{mm} become larger than

1, because they are $\mathcal{O}(Z)/k_m$. Thus the first anomaly, referred as Rayleigh Wood anomaly, corresponds to

$$\text{(i)} \quad k_m = 0, \begin{cases} \mathsf{R}_{n\neq m} \simeq -\dfrac{\mathsf{z}_{n0}}{\mathsf{z}_{mm}} \to 0, \\ \mathsf{R}_m \simeq -\dfrac{\mathsf{z}_{m0}}{\mathsf{z}_{mm}} \to \mathcal{O}(1). \end{cases} \tag{25}$$

Now, because $\mathsf{z}_{mm} \propto 1/k_m$ increases, it is susceptible to produce $1+\mathsf{z}_{mm}=0$ if z_{mm} is real negative. This is possible from Eq. (17) if the mode m is evanescent (in this case, the quantities ik/k_m, α_{mm} and Z are real positive, producing z_{mm} real negative). Thus, the second Wood anomaly appears below the cut off frequency of the mode m and leads to

$$\text{(ii)} \quad 1+\mathsf{z}_{mm}=0, \;\; ik_m<0, \quad \mathsf{R}_n \simeq -\frac{\mathsf{z}_{n0}}{\sum\limits_{j\neq m}\mathsf{z}_{jj}} \to \mathcal{O}(1). \tag{26}$$

This confirms qualitatively that our expressions Eqs. (24) are able to predict the occurrence of anomalies.

3.3 More quantitative estimate of the solution at the anomalies

Near $k_m = 0$ and $1+\mathsf{z}_{mm}=0$, at least one of the terms in z deviate from a $\mathcal{O}(Z)$; this makes our estimate of R in Eq. (24) *a priori* suspicious. Let us come back to the exact system (15), that is re-written as

$$\begin{cases} \left[1+\dfrac{1}{\mathsf{z}_{00}}\right]\mathsf{R}_0 + \displaystyle\sum_{j\neq 0}\frac{\mathsf{z}_{0j}}{\mathsf{z}_{00}}\mathsf{R}_j = -1, \\ \mathsf{R}_0 + \dfrac{1}{\mathsf{z}_{n0}}\mathsf{R}_n + \displaystyle\sum_{j\neq 0}\frac{\mathsf{z}_{nj}}{\mathsf{z}_{n0}}\mathsf{R}_j = -1, \quad \text{for } n\neq 0 \end{cases} \tag{27}$$

As previously said, solving exactly the above system is possible owing to the expression of z for any truncation N. Now, if we assume that the truncation N is small enough, so that all the shape factor roughly equal unity ($kL, k_N L \ll 1$), a huge simplification occurs. Indeed, in that case, we have for $j\neq 0$

$$\frac{\mathsf{z}_{0j}}{\mathsf{z}_{00}} = \frac{\mathsf{z}_{nj}}{\mathsf{z}_{n0}} = \sqrt{2}(-1)^j. \tag{28}$$

It follows that the sum $S_1 \equiv \sum_{j\neq 0}(\mathsf{z}_{nj}/\mathsf{z}_{n0})\mathsf{R}_j$ does not depend on n. Thus, we get from the Eqs. (27)

$$\mathsf{R}_n = \frac{\mathsf{z}_{n0}}{\mathsf{z}_{00}}\mathsf{R}_0, \tag{29}$$

afterwards any of the Eqs. (27) gives

$$\left[1+\sum_j \frac{\mathsf{z}_{j0}\mathsf{z}_{0j}}{\mathsf{z}_{00}}\right]\mathsf{R}_0 = -\mathsf{z}_{00}. \tag{30}$$

Eq. (28) for $n=j$ gives $\mathsf{z}_{j0}\mathsf{z}_{0j}/\mathsf{z}_{00} = \mathsf{z}_{jj}$. Thus, ironically, the above expression of R_n valid for a sum truncated to small N (and owing to the property (28)) coincides with the expression Eq. (24), valid for small z, but where the sum can be extended to an infinite number of terms (when accounted for the factors of shape).

This tells us that we can be more confident in inspecting the behavior of the R_n at the anomalies using explicitly

$$\mathsf{R}_n \simeq \frac{iZ/2\,\sqrt{2-\delta_{n0}}(-1)^n k/k_n}{1-iZ/2\left[1+2\displaystyle\sum_{j\neq 0}k/k_j\right]}. \tag{31}$$

(i) In the vicinity of $k_m = 0$. In this case, the denominator is $-iZk/k_m$ at dominant order since k_m can be much smaller than Z, from which we deduce

$$\mathsf{R}_n \simeq 0, \text{for } n\neq m, \text{ and } \mathsf{R}_m \simeq \frac{(-1)^{m-1}}{\sqrt{2}}. \tag{32}$$

(ii) In the vicinity of $1+\mathsf{z}_{mm}=0$, the wavenumber is $k/k_m \simeq 1/(iZ)$, thus k is close to $m\pi/h$, and

$$\mathsf{R}_n \simeq -\sqrt{2-\delta_{n0}}(-1)^n \frac{k/k_n}{1+2\displaystyle\sum_{j\neq 0,m}k/k_j}. \tag{33}$$

In the following Section, this is confirmed quantitatively by comparison with direct numerical calculations. In the case of TM waves, no anomalies are obtained (the calculations are collected in Appendix A).

4 RESULTS

Results presented in this Section concern TE waves (s-polarized). We performed direct numerical calculations using a multimodal method [10], similar to the RCWA [11]. The scatterers are square ($h_s = L$) with $h_s/h = 0.1$; the frequency range is such that the non dimensional frequency $kh/2\pi$ varies between 0 and 3.3, thus passing through 3 cutoff frequencies at integer values of $kh/2\pi$. The scatterers have permittivity $\epsilon = 4$. This produces a scattering strength Z in Eq. (18) increasing with frequency, from 0 to about 0.6. Figures 2 show the wave fields at the two anomalies just below ($kh/2\pi = 0.9821$) and at the first cut off frequency ($kh/2\pi = 1$). At the first anomaly, only the mode 0 is propagating; from the direct numerics, we get a reflection coefficient $\mathsf{R}_0 \simeq -1$ (the transmission coefficient has an amplitude 10^{-4}); the plane wave is totally reflected while the mode 2, excited with high amplitude, is dominant in the near field. At the cut of

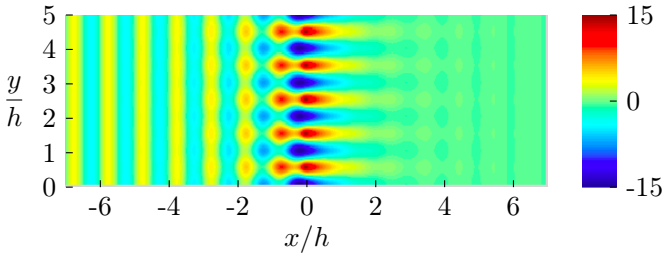

(a) $kh/2\pi = 0.9821$

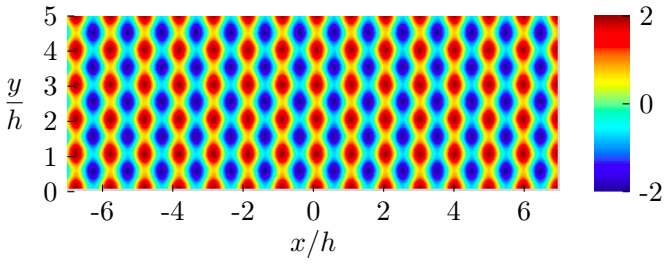

(b) $kh/2\pi = 1$

FIG. 2 Wavefield E (imaginary part) around the row of square scatterers (at $x=0$) at the two anomalies below and at the first cutoff frequency $kh/2\pi = 1$. The scatterer size is $h_s = L = h/10$ and $\epsilon = 4$.

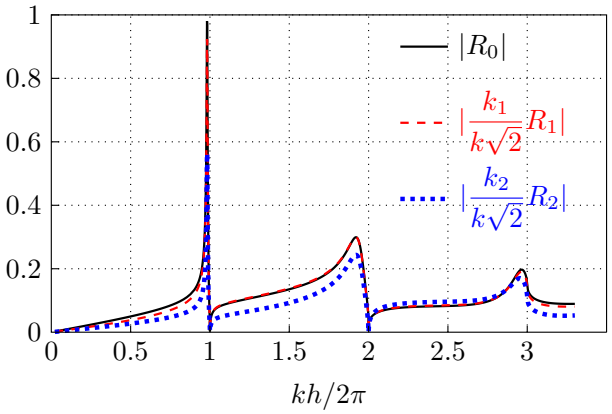

FIG. 3 Amplitude of the reflection coefficient R_0 and, for comparison, $|(k_1/k\sqrt{2})R_1|$ and $|(k_2/k\sqrt{2})R_2|$ (see Eq. (29)). The three coefficients R_n have been calculated using full wave simulations.

frequency, the mode 0 has $|R_0| \simeq 0.0032$ while $|R_1| \simeq 0.7070$, very close to $1/\sqrt{2}$, as predicted in Eq. (32). By energy conservation, the transmission coefficient has an amplitude unity. The pattern is simply the superposition of the incident wave $e^{2i\pi x/h}$ and the field due to the excitation of the mode 2 with amplitude 1, namely $\cos 2\pi y/h$.

In Figure 3, we inspect the validity of the property (29). With $z_{n0}/z_{00} \simeq \sqrt{2}(-1)^n k/k_n$, we report the reflection coefficient R_0 as a function of the non dimensional frequency $kh/2\pi$ and compare it to $(k_n/k\sqrt{2})R_n$, $n = 1,2$. The property is reasonably satisfied, in fact unexpectedly well above the second cut off frequency where the two assumptions of weak scattering and small scatterer size are questionable. The reflection coefficients of the mode 1 and 2 are represented in the evanescent regime, below their cut-off frequencies.

Finally, we report in Figure 4 the reflection coefficients of the mode 0 (n = 0) and 2 (n = 1) as a function of $kh/2\pi$. The values obtained numerically (blue circles) are compared with 3 estimations. To simplify the discussion, we used for the three estimations the exact solutions z in Eqs. (19) of the linearized Riccati equation (16). Then, these estimates are based on the resolution of the system Eq. (15) and can be sorted by increasing complexity: $R_n^{(0)} \equiv -z_{n0}$ (green dotted curves) is the most simple linearization, $R_n^{(1)}$ (red curves) the linearization of both the numerator and denominator of the solution, Eq. (24), and $R_n^{(2)}$ (black dashed curves) the numerical inversion of Eq. (15). In the two last cases, we used $N = 20$, for which the solutions are converged. $R_n^{(0)}$ is as one expects: able to describe the smooth and small variations but missing the rapid ones. The most remarkable fact is the similarity between $R_n^{(1)}$ and $R_n^{(2)}$. This tells us that the main error in our prediction is attributable to the linearization of the Riccati equation (the unique source of error in $R_n^{(2)}$, exact solution of (15), is the value of z). This has been confirmed by integrating numerically the full Riccati equation (13) to get z, and by using then these z values to get the reflection coefficients from our approximate expression Eq. (24). The resulting error when compared to the reflection coefficients issued from full numerics (error calculated for the 3 first modes) is lower than 5% in the whole frequency range. The results for the first two modes are shown in Figure 5. To repeat

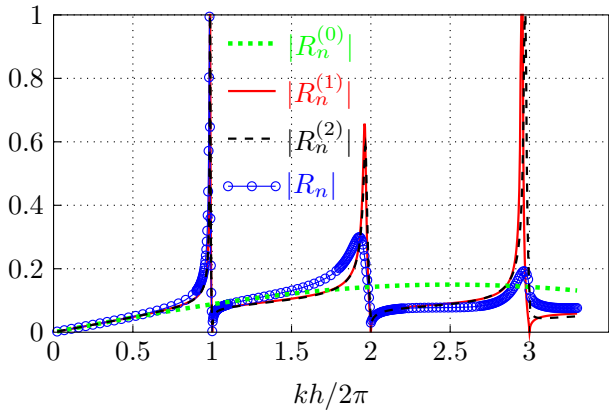

(a) $n = 0$

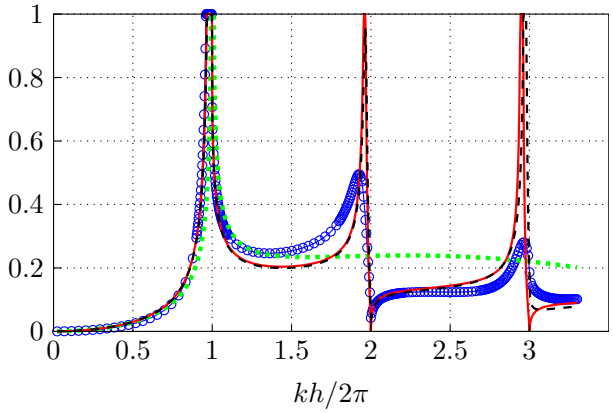

(b) $n = 1$

FIG. 4 Reflection coefficients (a) $|R_0|$ and (b) $|R_1|$ as function of the frequency, calculated with full wave numerics (blue circles), and comparison with the rough estimate $R_n^{(0)} = -z_{n0}$ (green dotted curve), $R_n^{(1)}$ obtained from Eq. (24) using Eq. (19) (red curve), and $R_n^{(2)}$ obtained by numerical inversion of (15) using Eq. (19). The maximum value of $|R_1|$ is 5.2 at $kh/2\pi \simeq 0.9818$.

our main conclusion, the difference in agreement between the blue curves in Figure 5 and in Figure 4 is the resolution of z, including or neglecting respectively the non linear term in the Riccati equation.

5 CONCLUSION

The scattering of light by an array of small dielectric scatterers has been studied. For s-polarized waves, anomalies in the behavior of the reflection coefficients are observed, similar to Wood's anomalies for metallic gratings. We develop an analysis based on a modal formulation and the use of the admittance matrix, governed by a non linear differential equation (the Riccati equation). The reflection coefficients can be determined by inversion of a matrix system involving the admittance. An estimate of the reflection coefficients is proposed using two approximations: (i) the resolution of the Riccati equation after linearization, (ii) the explicit inversion of the matrix system on the reflection coefficients in the weak scattering approximation. Comparison with direct numerical calculations shows that the main source of error in our expression of R is the linearization of the Riccati equation. Works are in progress to propose more accurate solutions of the non linear Riccati equation.

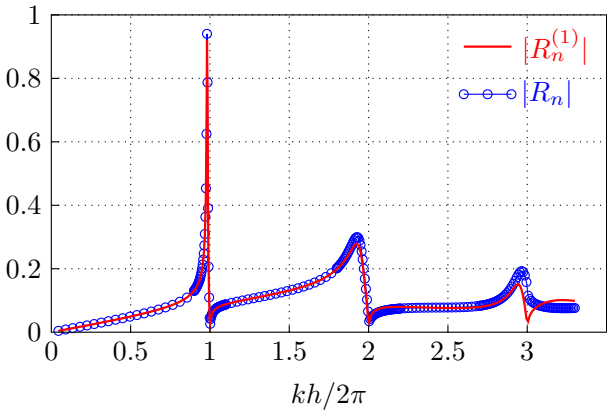

(a) $n = 0$

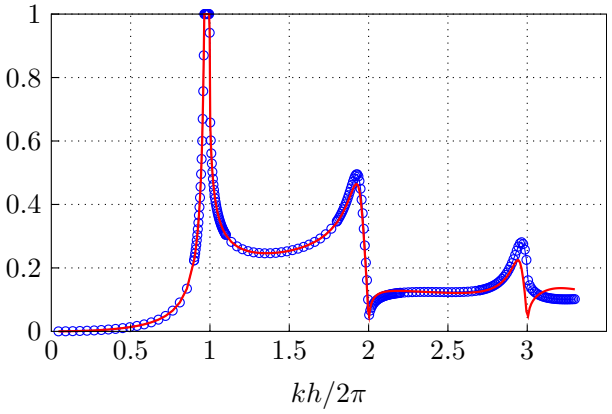

(b) $n = 1$

FIG. 5 Same representation as in Figure 4: here the red curve shows the reflection coefficient given by Eq. (23) using z calculated numerically by integrating the full Riccati equation (13).

6 ACKNOWLEDGEMENTS

This work has been supported by the Agence Nationale de la Recherche, through the grant ANR ProCoMedia, project ANR-10-INTB-0914.

APPENDIX

A THE CASE OF TM WAVES

We show in this appendix that the solution of the scattering problem at dominant order does not exhibit any anomaly for TM waves. Here, the weak representation, Eq. (2), is

$$\int_\Omega \mathrm{d}\mathbf{r}\left[\nabla H\cdot\nabla\tilde{H}-k^2H\tilde{H}\right]+\int_{\Omega_0}\mathrm{d}\mathbf{r}\left(\frac{1}{\epsilon}-1\right)\nabla H\cdot\nabla\tilde{H}=0, \quad (34)$$

where $\tilde{H}(\mathbf{r}) = \tilde{H}(x)\varphi_n(y)$ is a test function compactly supported. After expansion $H(x,y) = \sum H_m(x)\varphi_m(y)$, we get

$$\partial_x\left[H_n'+\left(\frac{1}{\epsilon}-1\right)\mathsf{C}_{nm}H_m'\right]+k_n^2H_n-\left(\frac{1}{\epsilon}-1\right)\mathsf{D}_{nm}H_m=0, \quad (35)$$

with

$$\mathsf{D}_{nm}(x)\equiv\int_{(h-h_s)/2}^{(h+h_s)/2}\mathrm{d}y\,\varphi_n'(y)\varphi_m'(y), \quad (36)$$

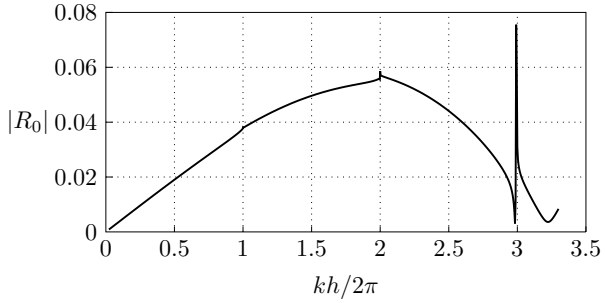

FIG. 6 Reflection coefficient $|R_0|$ in the same configuration as in Section 4, but for p-polarized waves.

We now define the quantity $G_n \equiv H_n' + (1/\epsilon - 1)\mathsf{C}_{nm}H_m'$ and

$$\begin{pmatrix}\mathbf{H}\\ \mathbf{G}\end{pmatrix}'=\begin{pmatrix}0 & \mathsf{N}^{-1}\\ \mathsf{K}^2+\mathsf{M} & 0\end{pmatrix}\begin{pmatrix}\mathbf{H}\\ \mathbf{G}\end{pmatrix} \quad (37)$$

with

$$\begin{cases}\mathsf{N}(x)\equiv\mathsf{I}+(1/\epsilon-1)\mathsf{C}(x),\\ \mathsf{M}(x)\equiv(1/\epsilon-1)\mathsf{D}(x).\end{cases} \quad (38)$$

and the admittance matrix, defined as $\mathbf{G} = \mathsf{Y}\mathbf{H}$, satisfies

$$\mathsf{Y}' = -\mathsf{Y}\mathsf{N}^{-1}\mathsf{Y}+\mathsf{K}^2+\mathsf{M}. \quad (39)$$

If weak scattering is assumed, the - small - change in the admittance $\mathsf{z} \equiv \mathsf{K}^{-1}(\mathsf{Y}-\mathsf{K})/2$ satisfies the differential equation

$$\mathsf{z}_{nm}' = -i(k_n+k_m)\mathsf{z}_{nm}+(1/\epsilon-1)\times\left[\mathsf{D}_{nm}-k_nk_m\mathsf{C}_{nm}\right]/(2ik_n). \quad (40)$$

where we have used $\mathsf{N}^{-1} \simeq \mathsf{I} - (1/\epsilon - 1)\mathsf{C}$ for N close to the identity matrix. We get, for small scatterer size,

$$\mathsf{z}_{nm} = i\alpha_{nm}\frac{k_n}{k}Z, \quad (41)$$

with α_{nm} defined in Eq. (18) and with the scattering strength is now $Z \equiv (1/\epsilon - 1)kLh_s/h$. Obviously, z is now always $\mathcal{O}(Z)$ from which we deduce that no anomalies occurs in this case.

Figure 6 shows the reflection coefficient R_0 in the same configuration as in Section 4, but for p-polarized waves. It is visible that the anomalies are much smoother except at the third cut off frequency at $kh = 6\pi$. At this high frequency, the estimate of z in Eq. (41) is inaccurate and a complete calculation for $kL \sim 1$ would be necessary.

References

[1] A. Hessel, and A. A. Oliner, "A new theory of Wood's anomalies on optical gratings," Appl. Optics **4**, 1275–1297 (1965).

[2] U. Fano, "The theory of anomalous diffraction gratings and of quasi-stationary waves on metallic surfaces (Sommerfeld's waves)," J. Opt. Soc. Am. **31**, 213–222 (1941).

[3] B. M. Bolotovskii, and A. N. Lebedev, "On threshold phenomena in classical electrodynamics," Sov. Phys. JETP **26(4)**, 784–786 (1968).

[4] B. M. Bolotovskii, and K. I. Kugel, "Contribution to the theory of threshold phenomena in diffraction of electromagnetic wave," Sov. Phys. JETP **30(1)**, 95–99 (1970).

[5] D. Maystre, *Theory of Wood's anomalies* (Springer, Berlin, Heidelberg, 2012).

[6] J. B. Titchener, and J. R. Willis, "The reflection of electromagnetic waves from stratified anisotropic media," IEEE T. Antenn. Propag. **39**, 35–39 (1991).

[7] G. Caviglia, and A. Morro, "Riccati equations for wave propagation in planarly-stratified solids," Eur. J. Mech. A-Solid **19**, 721–741 (2000).

[8] A. B. Akimov, N. A. Gippius, and S. G. Tikhodeev, "Optical Fano resonances in photonic crystal slabs near the diffraction threshold anomalies," JETP Lett. **93(8)**, 427–430 (2011).

[9] A. Maurel, and J.-F. Mercier, "Propagation of guided waves through weak penetrable scatterers," J. Acoust. Soc. Am. **131**, 1874–1889 (2012), [Erratum: J. Acoust. Soc. Am. 132, 1230 (2012)].

[10] A. Maurel, J.-F. Mercier, and S. Félix, "Wave propagation through penetrable scatterers in a waveguide and through a penetrable grating," J. Acoust. Soc. Am. (to appear).

[11] M. G. Moharam, and T. K. Gaylord, "Rigorous coupled wave analysis of planar-grating diffraction," J. Opt. Soc. Am. **71**, 811–818 (1981).